ISSN: 0067-2904

Influence of MHD and Wall Properties on the Peristaltic Transport of a Williamson Fluid with Variable Viscosity Through Porous Medium

Dheia G. Salih Al-Khafajy
Department of Mathematics, Faculty of Computer Science and Information Technology, University of Al-Qadisiyah, Diwaneyah, Iraq.

Abstract

This paper concerns the peristaltic flow of a Williamson fluid with variable viscosity model through porous medium under combined effects of MHD and wall properties. The assumptions of Reynolds number and long wavelength is investigated. The flow is investigated in a wave frame of reference moving with velocity of the wave. The perturbation series in terms of the Weissenberg number (We <1) was used to obtain explicit forms for velocity field and stream function. The effects of thermal conductivity, Grashof number, Darcy number, magnet, rigidity, stiffness of the wall and viscous damping force parameters on velocity and stream function have been studied.

Keywords: MHD, Peristaltic transport, Williamson fluid with variable viscosity model, Porous medium.

تأثير الهايدروداينامیكا الممغنطة وخصائص الجدار على الانتقال التموجي لمائع وليمسون ذو اللزوجة المتغيرة خلال وسط مسامي

ضياء غازي صالح الخفاجي
قسم الرياضيات، كلية علوم الحاسوب وتكنولوجيا المعلومات ، جامعة القادسية ، الديوانية ، العراق.

الخلاصة

في هذا البحث، درسنا التدفق التموجي لمائع وليمسون ذي اللزوجة المتغيرة خلال قناة مسامية تحت تأثير الهايدروداينامیكا الممغنطة وخصائص الجدار. افترضنا عدد رينولد وطول الموجة صغيران جداً. ان التدفق يتحرك بشكل موجة مسند بسرعة الموجة . استخدمنا طريقة سلسلة الاضطراب لحل المعادلات التفاضلية باعتماد عدد وزنبرك (We<1) للحصول على توضيح لحقل السرعة ودالة التدفق. درسنا تاثير التوصيل الحراري، عدد كرشوف، عدد دارسي، المغناطيسية، تصلب الجدار وقوة اضمحلال اللزوجة على حقل السرعة ودالة التدفق.

1. Introduction

Peristaltic flows have attracted the interest of a number of researchers because of wide applications in physiology and industry. Particularly, the occurrence of such flows are quite prevalent in biological

Email: dheia.salih@qu.edu.iq

organs. Since, the pioneering works of [1]. A number of analytical, numerical and experimental [2-6] studies of peristaltic flows of different fluids have been reported under different conditions with reference to physiological and mechanical situations.

Several researchers considered the fluid to behave like a Newtonian fluid for physiological peristalsis including the flow of blood in arterioles. But such a model cannot be suitable for blood flow unless the non-Newtonian nature of the fluid is included in it. The non-Newtonian peristaltic flow using a constitutive equation for a second order fluid has been investigated by [7] for a planar channel and by [8] for an axisymmetric tube. The effects of third order fluid on peristaltic transport in a planar channel were studied by [9] and the corresponding axisymmetric tube results were obtained by [10]. [11] studied peristaltic transport of third order fluid in an asymmetric channel. Peristaltic motion of a Williamson fluid in an asymmetric channel was studied by [12].

Further an interesting fact is that in oesophagus, the movement of food is due to peristalsis. The food moves from mouth to stomach even when upside down. Oesophagus is a long muscular tube commences at the neck opposite the long border of cricoids cartilage and extends from the lower end of the pharynx to the cardiac orifice of the stomach. The swallowing of the food bolus takes place due to the periodic contraction of the esophageal wall. Pressure due to reflexive contraction is exerted on the posterior part of the bolus and the anterior portion experiences relaxation so that the bolus moves ahead. The contraction is practically not symmetric, yet it contracts to zero lumen and squeezes it marvelously without letting any part of the food bolus slip back in the opposite direction. This shows the importance of peristalsis in human beings. [13] studied the influence of wall properties on the Poiseuille flow under peristalsis. Mathematical model for the esophageal swallowing of a food bolus is analyzed by [14]. [15] analysed the peristaltic flow of a micropolar fluid in a vertical channel with longwave length approximation. [16] studied the influence of wall properties on peristaltic transport with heat transfer. [17] studied the influence of wall properties on MHD peristaltic transport of dusty fluid. A new model for study the effect of wall properties on peristaltic transport of a viscous fluid has been investigated by [18], [19] studied the effect of slip, wall properties and heat transfer on MHD peristaltic transport. Recently, [20-22], analyzed the Effects of MHD and wall properties on the peristaltic transport of a various fluids through porous medium channel.

Motivated by this, we consider the peristaltic flow of a Williamson fluid with variable viscosity model through porous medium under combined effects of MHD and wall properties. The results are analyzed for different values of parameters namely Grashof number, Darcy number, thermal conductivity, magnet, rigidity, stiffness and viscous damping forces of the channel wall through porous medium.

2. MATHEMATICAL FORMULATION

Consider the peristaltic flow of an incompressible Williamson fluid in a flexible channel with flexible induced by sinusoidal wave trains propagating with constant speed c along the channel walls.

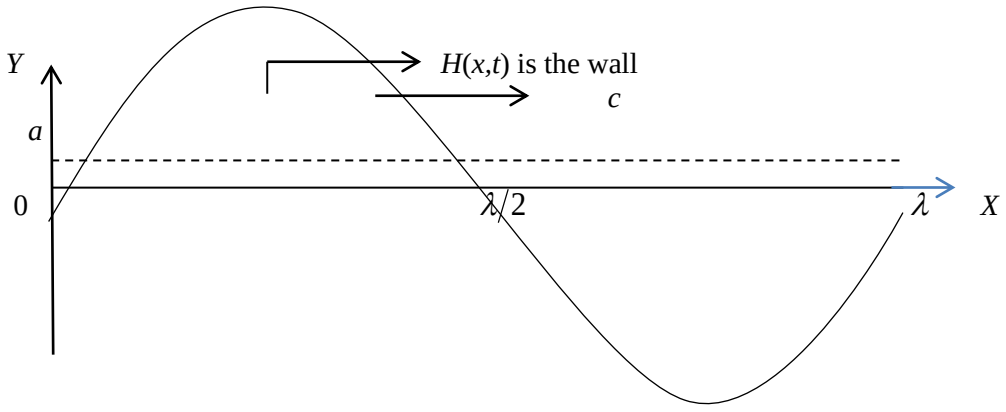

Figure 1- Geometry of the problem

The wall deformation is given by

$$H(\bar{x},\bar{t}) = a - \bar{\phi}\cos^2\frac{\pi}{\lambda}(\bar{x} - c\bar{t}) \quad (1)$$

where $\overline{h}$, $\overline{x}$, $\overline{t}$, $\overline{\phi}$, λ and c represent transverse vibration of the wall, axial coordinate, time, half width of the channel, amplitude of the wave, wavelength and wave velocity respectively.
The basic equations governing the non-Newtonian incompressible Williamson fluid are given by: The continuity equation is given by:

$$\frac{\partial \overline{u}}{\partial \overline{x}} + \frac{\partial \overline{v}}{\partial \overline{y}} + \frac{\partial \overline{w}}{\partial \overline{z}} = 0, \tag{2}$$

The momentum equations are:

$$\rho\left(\frac{\partial \overline{u}}{\partial \overline{t}} + \overline{u}\frac{\partial \overline{u}}{\partial \overline{x}} + \overline{v}\frac{\partial \overline{u}}{\partial \overline{y}} + \overline{w}\frac{\partial \overline{u}}{\partial \overline{y}}\right) = -\frac{\partial \overline{p}}{\partial \overline{x}} + \frac{\partial \overline{\tau}_{\overline{xx}}}{\partial \overline{x}} + \frac{\partial \overline{\tau}_{\overline{xy}}}{\partial \overline{y}} + \frac{\partial \overline{\tau}_{\overline{xz}}}{\partial \overline{z}} + \rho g\alpha(T - T_0) - \sigma B_0^2 \overline{u} - \frac{\mu(T)}{k}\overline{u} \tag{3}$$

$$\rho\left(\frac{\partial \overline{v}}{\partial \overline{t}} + \overline{u}\frac{\partial \overline{v}}{\partial \overline{x}} + \overline{v}\frac{\partial \overline{v}}{\partial \overline{y}} + \overline{w}\frac{\partial \overline{v}}{\partial \overline{z}}\right) = -\frac{\partial \overline{p}}{\partial \overline{y}} + \frac{\partial \overline{\tau}_{\overline{yx}}}{\partial \overline{x}} + \frac{\partial \overline{\tau}_{\overline{yy}}}{\partial \overline{y}} + \frac{\partial \overline{\tau}_{\overline{yz}}}{\partial \overline{z}} - \frac{\mu(T)}{k}\overline{v} \tag{4}$$

$$\rho\left(\frac{\partial \overline{w}}{\partial \overline{t}} + \overline{u}\frac{\partial \overline{w}}{\partial \overline{x}} + \overline{v}\frac{\partial \overline{w}}{\partial \overline{y}} + \overline{w}\frac{\partial \overline{w}}{\partial \overline{z}}\right) = -\frac{\partial \overline{p}}{\partial \overline{y}} + \frac{\partial \overline{\tau}_{\overline{zx}}}{\partial \overline{x}} + \frac{\partial \overline{\tau}_{\overline{zy}}}{\partial \overline{y}} + \frac{\partial \overline{\tau}_{\overline{zz}}}{\partial \overline{z}} \tag{5}$$

The temperature equation is given by:

$$\rho c_p\left(\frac{\partial T}{\partial \overline{t}} + \overline{u}\frac{\partial T}{\partial \overline{x}} + \overline{v}\frac{\partial T}{\partial \overline{y}} + \overline{w}\frac{\partial T}{\partial \overline{z}}\right) = K\left(\frac{\partial^2 T}{\partial \overline{x}^2} + \frac{\partial^2 T}{\partial \overline{y}^2} + \frac{\partial^2 T}{\partial \overline{z}^2}\right) + \Phi \tag{6}$$

where $\overline{u}$ is the axial velocity, $\overline{v}$ transverse velocity, $\overline{y}$ transverse coordinate, ρ fluid density, $\overline{p}$ pressure, μ_0 fluid viscosity, g acceleration due to gravity, α coefficient of linear thermal expansion of fluid, B_0 magnetic parameter, T temperature, c_p specific heat at constant pressure, k is the thermal conductivity and Φ constant heat addition/absorption.

The velocity and temperatures at the central line and the wall of the peristaltic channel are given as:

$\frac{\partial \overline{u}}{\partial \overline{y}} = 0$, $T = T_0$ at $\overline{y} = 0$

$\overline{u} = 0$, $T = T_1$ at $\overline{y} = \overline{h}$

where T_0 is the temperature at centre is line and T_1 is the temperature on the wall of peristaltic channel.

The constitutive equation for a Williamson fluid model [4], is

$$\overline{\tau} = -[\mu_\infty + (\mu(T) + \mu_\infty)(1 - \Gamma\dot{\overline{\gamma}})^{-1}]\dot{\overline{\gamma}} \tag{7}$$

where τ is the extra stress tensor, μ_∞ is the infinite shear rate viscosity, μ_0 is the zero shear rate viscosity, Γ is the time constant and $\dot{\gamma}$ is defined as

$$\dot{\gamma} = \sqrt{\frac{1}{2}\sum_i\sum_j \dot{\gamma}_{ij}\dot{\gamma}_{ji}} = \sqrt{\frac{1}{2}\Pi} \tag{8}$$

Here Π is the second invariant stress tensor. We consider in the constitutive equation (7) the case for which $\mu_\infty = 0$ and $\Gamma < 1$ so we can write

$$\overline{\tau} = -\mu(T)(1 + \Gamma\dot{\overline{\gamma}})]\dot{\overline{\gamma}} \tag{9}$$

The above model reduces to Newtonian for $\Gamma = 0$.

The governing equation of motion of the flexible wall may be expressed as:

$$L^* = \overline{p} - \overline{p}_0 \tag{10}$$

where L^* is an operator, which is used to represent the motion of stretched membrane with viscosity damping forces such that

$$L^* = -\kappa\frac{\partial^2}{\partial x^2} + m_1\frac{\partial^2}{\partial t^2} + C\frac{\partial}{\partial t} \tag{11}$$

where κ is the elastic tension in the membrane, m_1 is the mass per unit area, *C* is the coefficient of viscous damping forces.

Continuity of stress at $y = \bar{h}$ and using momentum equation, yield

$$\frac{\partial}{\partial \bar{x}} L^*(\bar{h}) = \frac{\partial \bar{p}}{\partial \bar{x}} = \frac{\partial \bar{\tau}_{\bar{x}\bar{x}}}{\partial \bar{x}} + \frac{\partial \bar{\tau}_{\bar{x}\bar{y}}}{\partial \bar{y}} + \frac{\partial \bar{\tau}_{\bar{x}\bar{z}}}{\partial \bar{z}} - \rho\left(\frac{\partial \bar{u}}{\partial \bar{t}} + \bar{u}\frac{\partial \bar{u}}{\partial \bar{x}} + \bar{v}\frac{\partial \bar{u}}{\partial \bar{y}} + \bar{w}\frac{\partial \bar{u}}{\partial \bar{z}}\right) + \rho g\alpha(T - T_0) - \sigma B_0^2 \bar{u} - \frac{\mu(T)}{k}\bar{u} \tag{12}$$

3. Method of solution

Let $\bar{u}$ and $\bar{v}$ be the respective velocity components in the radial and axial directions in the fixed frame, respectively.

For the unsteady two-dimensional flow, the velocity components may be written as follows:

$$\bar{V} = (\bar{u}(\bar{x}, \bar{y}), \bar{v}(\bar{x}, \bar{y}), 0) \tag{13}$$

The temperature function may be written as follows:

$$T = T(x, y). \tag{14}$$

The equations of motion (2)-(6), the equation (12), take the form:

$$\frac{\partial \bar{u}}{\partial \bar{x}} + \frac{\partial \bar{v}}{\partial \bar{y}} = 0, \tag{15}$$

$$\rho\left(\frac{\partial \bar{u}}{\partial \bar{t}} + \bar{u}\frac{\partial \bar{u}}{\partial \bar{x}} + \bar{v}\frac{\partial \bar{u}}{\partial \bar{y}}\right) = -\frac{\partial \bar{p}}{\partial \bar{x}} + \frac{\partial \bar{\tau}_{\bar{x}\bar{x}}}{\partial \bar{x}} + \frac{\partial \bar{\tau}_{\bar{x}\bar{y}}}{\partial \bar{y}} + \rho g\alpha(T - T_0) - \sigma B_0^2 \bar{u} - \frac{\mu(T)}{k}\bar{u}, \tag{16}$$

$$\rho\left(\frac{\partial \bar{v}}{\partial \bar{t}} + \bar{u}\frac{\partial \bar{v}}{\partial \bar{x}} + \bar{v}\frac{\partial \bar{v}}{\partial \bar{y}}\right) = -\frac{\partial \bar{p}}{\partial \bar{y}} + \frac{\partial \bar{\tau}_{\bar{y}\bar{x}}}{\partial \bar{x}} + \frac{\partial \bar{\tau}_{\bar{y}\bar{y}}}{\partial \bar{y}} - \frac{\mu(T)}{k}\bar{v}, \tag{17}$$

$$\rho c_p\left(\frac{\partial T}{\partial \bar{t}} + \bar{u}\frac{\partial T}{\partial \bar{x}} + \bar{v}\frac{\partial T}{\partial \bar{y}}\right) = K\left(\frac{\partial^2 T}{\partial \bar{x}^2} + \frac{\partial^2 T}{\partial \bar{y}^2}\right) + \Phi, \tag{18}$$

$$\frac{\partial}{\partial \bar{x}} L^*(\bar{h}) = \frac{\partial \bar{p}}{\partial \bar{x}} = \frac{\partial \bar{\tau}_{\bar{x}\bar{x}}}{\partial \bar{x}} + \frac{\partial \bar{\tau}_{\bar{x}\bar{y}}}{\partial \bar{y}} - \rho\left(\frac{\partial \bar{u}}{\partial \bar{t}} + \bar{u}\frac{\partial \bar{u}}{\partial \bar{x}} + \bar{v}\frac{\partial \bar{u}}{\partial \bar{y}}\right) + \rho g\alpha(T - T_0) - \sigma B_0^2 \bar{u} - \frac{\mu(T)}{k}\bar{u} \tag{19}$$

In order to simplify the governing equations of the motion, we may introduce the following dimensionless transformations as follows:

$$\left.\begin{aligned} &x = \frac{\bar{x}}{\lambda}, y = \frac{\bar{y}}{a}, \delta = \frac{a}{\lambda}, u = \frac{\bar{u}}{c}, v = \frac{\bar{v}}{c\delta}, t = \frac{c\bar{t}}{\lambda}, \phi = \frac{\bar{\phi}}{a}, We = \frac{\Gamma c}{a}, Gr = \frac{gpa^2\alpha(T_1 - T_0)}{c\mu_0}, \\ &p = \frac{a^2\bar{p}}{\mu_0 \lambda c}, \vartheta = \frac{T - T_0}{T_1 - T_0}, \mu(\vartheta) = \frac{\mu(T)}{\mu_0}, Da = \frac{k}{a^2}, M^2 = \frac{\sigma B_0^2 a^2}{\mu_0}, \beta = \frac{a^2\Phi}{K(T_1 - T_0)}, \\ &\mathrm{Re} = \frac{\rho c a}{\mu_0}, \mathrm{Pr} = \frac{\mu_0 c_p}{K}, \tau_{xx} = \frac{\lambda}{\mu_0 c}\bar{\tau}_{\bar{x}\bar{x}}, \tau_{xy} = \frac{a}{\mu_0 c}\bar{\tau}_{\bar{x}\bar{y}}, \tau_{yy} = \frac{\lambda}{\mu_0 c}\bar{\tau}_{\bar{y}\bar{y}}, \dot{\gamma} = \frac{a\bar{\dot{\gamma}}}{c} \end{aligned}\right\} \tag{20}$$

where δ is the length of the channel, *We* Weissenberg number, *Da* Darcy number, Re Reynolds number, *Gr* Grashof number, θ dimensionless temperature, *M* magnetic parameter, β dimensionless heat source/sink parameter and Pr Prandtl number.

Substituting (20) into a governing equation, we obtain the following non-dimensional equations and boundary conditions:

$$h(x,t) = 1 - \phi\cos^2\pi(x - t) \tag{21}$$

$$\frac{\partial u}{\partial x} + \frac{\partial v}{\partial y} = 0 \tag{22}$$

$$\mathrm{Re}\,\delta\left(\frac{\partial u}{\partial t} + u\frac{\partial u}{\partial x} + v\frac{\partial u}{\partial y}\right) = -\frac{\partial p}{\partial x} + \delta^2\frac{\partial \tau_{xx}}{\partial x} + \frac{\partial \tau_{xy}}{\partial y} + Gr\vartheta - M^2 u - \frac{\mu(\vartheta)}{Da}u \tag{23}$$

$$\mathrm{Re}\,\delta^3\left(\frac{\partial v}{\partial t}+u\frac{\partial v}{\partial x}+v\frac{\partial v}{\partial y}\right)=-\frac{\partial p}{\partial y}+\delta^2\left(\frac{\partial \tau_{yx}}{\partial x}+\frac{\partial \tau_{yy}}{\partial y}\right)-\frac{\delta^2}{Da}\mu(\vartheta)v \tag{24}$$

$$\mathrm{Pr}\,\mathrm{Re}\,\delta\left(\frac{\partial}{\partial t}+u\frac{\partial}{\partial x}+v\frac{\partial}{\partial y}\right)\vartheta=\left(\delta^2\frac{\partial^2}{\partial x^2}+\frac{\partial^2}{\partial y^2}\right)\vartheta+\beta \tag{25}$$

$$E_1\frac{\partial^3 h}{\partial x^3}+E_2\frac{\partial^3 h}{\partial x\partial t^2}+E_3\frac{\partial^2 h}{\partial x\partial t}=\delta^2\frac{\partial \tau_{xx}}{\partial x}+\frac{\partial \tau_{xy}}{\partial y}-\mathrm{Re}\,\delta\left(\frac{\partial u}{\partial t}+u\frac{\partial u}{\partial x}+v\frac{\partial u}{\partial y}\right)+Gr\vartheta-M^2u-\frac{\mu(\vartheta)}{Da}u \tag{26}$$

where $E_1=-\dfrac{\kappa a^2}{\lambda^3\mu_0 c}$, $E_2=\dfrac{m_1 c a^2}{\lambda^3\mu_0}$, $E_3=\dfrac{Ca^2}{\lambda^2\mu_0}$

The constitutive relations equations (8)-(9) take the form:

$$\left.\begin{aligned}\tau_{xx}&=-2\mu(\vartheta)[1+We\dot\gamma]\frac{\partial u}{\partial x},\qquad \tau_{xy}=-\mu(\vartheta)[1+We\dot\gamma]\left(\frac{\partial u}{\partial y}+\delta^2\frac{\partial v}{\partial x}\right)\\ \tau_{yy}&=-2\mu(\vartheta)[1+We\dot\gamma]\frac{\partial v}{\partial y},\qquad \dot\gamma=\sqrt{2\delta^2\left(\frac{\partial u}{\partial x}\right)^2+\left(\frac{\partial u}{\partial y}+\delta^2\frac{\partial v}{\partial x}\right)^2+2\delta^2\left(\frac{\partial v}{\partial y}\right)^2}\end{aligned}\right\} \tag{27}$$

The corresponding boundary conditions are

$$\frac{\partial u}{\partial y}=0,\ v=0,\ \vartheta=0 \quad \text{at} \quad y=0 \tag{28}$$

$$u=0,\ \vartheta=1 \qquad \text{at} \quad y=h \tag{29}$$

The general solution of the governing equations (22)-(26) in the general case seems to be impossible; therefore, we shall confine the analysis under the assumption of small dimensionless wave number, it follows that $\delta << 1$. Along to this assumption, equations (22)-(26) become:

$$\frac{\partial u}{\partial x}+\frac{\partial v}{\partial y}=0 \tag{30}$$

$$\frac{\partial p}{\partial x}=\frac{\partial}{\partial y}\left(-\mu(\vartheta)[1+We\frac{\partial u}{\partial y}]\frac{\partial u}{\partial y}\right)+Gr\vartheta-M^2u-\frac{\mu(\vartheta)}{Da}u \tag{31}$$

$$\frac{\partial p}{\partial y}=0 \tag{32}$$

$$\frac{\partial^2\vartheta}{\partial y^2}+\beta=0 \tag{33}$$

$$\frac{\partial}{\partial y}\left(-\mu(\vartheta)[1+We\frac{\partial u}{\partial y}]\frac{\partial u}{\partial y}\right)+Gr\vartheta-M^2u-\frac{\mu(\vartheta)}{Da}u=E_1\frac{\partial^3 h}{\partial x^3}+E_2\frac{\partial^3 h}{\partial x\partial t^2}+E_3\frac{\partial^2 h}{\partial x\partial t} \tag{34}$$

The corresponding Stream function ($u=\partial\psi/\partial y, v=-\partial\psi/\partial x$) with boundary condition $\psi=0$ at $y=0$.

The exact solution of equation (33) with boundary condition given in equations (28)-(29) is

$$\vartheta=\frac{y}{h}+\frac{\beta}{2}(hy-y^2) \tag{35}$$

The Reynold's model of viscosity is used to describe the variation of viscosity with temperature

$$\mu(\vartheta)=e^{-\alpha\vartheta} \tag{36}$$

Using the Maclaurin series expansion, the above expression can be written as:

$$\mu(\vartheta)=1-\alpha\vartheta,\quad \alpha << 1 \tag{37}$$

Here $\alpha = 0$ corresponds to the constant viscosity case.

Compensating equation (37) into equation (34), we have:

$$\frac{\partial}{\partial y}\left(-(1-\alpha\vartheta)[1+We\frac{\partial u}{\partial y}]\frac{\partial u}{\partial y}\right)+Gr\vartheta-M^2u-\frac{(1-\alpha\vartheta)}{Da}u=E_1\frac{\partial^3 h}{\partial x^3}+E_2\frac{\partial^3 h}{\partial x\partial t^2}+E_3\frac{\partial^2 h}{\partial x\partial t} \tag{38}$$

4. Solution of the problem

Equation (32) shows that *p* dependents on *x* only. Equation (38) is a non-linear and it is difficult to get a closed form solution. However for vanishing *We* and α, the boundary value problem is agreeable to an easy analytical solution. In this case the equation becomes linear and can be solved. Nevertheless, small Γ suggests the use of perturbation technique to solve the non-linear problem. Accordingly, we write

$$\left.\begin{aligned} u &= u_0+Weu_1+We^2u_2+O(We^3)\\ \psi &= \psi_0+We\psi_1+We^2\psi_2+O(We^3)\end{aligned}\right\} \tag{39}$$

Substituting equations (39) into equation (38) with boundary conditions (20) and (21), then equating the like powers of *We*, we obtain

4-1 Zeroth-order system (We^0)

$$(1-\alpha\vartheta)\frac{\partial^2 u_0}{\partial y^2}-\alpha\frac{\partial\vartheta}{\partial y}\frac{\partial u_0}{\partial y}+\left(M^2+\frac{1}{Da}(1-\alpha\vartheta)\right)u_0=Gr\vartheta-\left(E_1\frac{\partial^3 h}{\partial x^3}+E_2\frac{\partial^3 h}{\partial x\partial t^2}+E_3\frac{\partial^2 h}{\partial x\partial t}\right) \quad \text{and}$$

$$\psi_0=\int u_0\,dy \tag{40}$$

4-2 First-order system (We^1)

$$(1-\alpha\vartheta)\frac{\partial^2 u_1}{\partial y^2}+2(1-\alpha\vartheta)\frac{\partial^2 u_0}{\partial y^2}\left(\frac{\partial u_0}{\partial y}\right)-\alpha\frac{\partial\vartheta}{\partial y}\frac{\partial u_1}{\partial y}-\alpha\frac{\partial\vartheta}{\partial y}\left(\frac{\partial u_0}{\partial y}\right)^2+\left[M^2+\frac{1}{Da}(1-\alpha\vartheta)\right]u_1=0$$

and $\psi_1=\int u_1\,dy$ (41)

4-3 Second-order system (We^2)

$$(1-\alpha\vartheta)\frac{\partial^2 u_2}{\partial y^2}+2(1-\alpha\vartheta)\left\{\frac{\partial^2 u_1}{\partial y^2}\frac{\partial u_0}{\partial y}+\frac{\partial^2 u_0}{\partial y^2}\frac{\partial u_1}{\partial y}\right\}-\alpha\frac{\partial\vartheta}{\partial y}\left\{\frac{\partial u_2}{\partial y}+2\frac{\partial u_1}{\partial y}\frac{\partial u_0}{\partial y}\right\}+\left[M^2+\frac{1}{Da}(1-\alpha\vartheta)\right]u_2=0$$

and $\psi_2=\int u_2\,dy$ (42)

The boundary conditions associated with the above equations are;

$$\frac{\partial u_0}{\partial y}=\frac{\partial u_1}{\partial y}=\frac{\partial u_2}{\partial y}=0,\ \ \psi_0=\psi_1=\psi_2=0 \quad \text{at} \quad y=0 \tag{43}$$

$$u_0=u_1=u_2=0, \quad \text{at} \quad y=h \tag{44}$$

In order to give some physical meaning to the problem we will consider the case only when α is small. Thus the above approximation equations have been obtained by the expansion in terms of *We*, and next we seek perturbations with parameters α.

If we substitute for u_i and ψ_i, (for i = 0, 1, 2) by the expression

$$\left.\begin{aligned} u_i &= u_{i0}+\alpha u_{i1}+\alpha^2u_{i2}+O(\alpha^3)\\ \psi_i &= \psi_{i0}+\alpha\psi_{i1}+\alpha^2\psi_{i2}+O(\alpha^3)\end{aligned}\right\} \tag{45}$$

and equate the coefficient of like powers in α, then the following set of equations are obtained

$$\begin{aligned}&(1-\alpha\vartheta)\frac{\partial^2}{\partial y^2}(u_{00}+\alpha u_{01}+\alpha^2u_{02})-\alpha\frac{\partial\vartheta}{\partial y}\frac{\partial}{\partial y}(u_{00}+\alpha u_{01}+\alpha^2u_{02})\\ &+\left(M^2+\frac{1}{Da}(1-\alpha\vartheta)\right)(u_{00}+\alpha u_{01}+\alpha^2u_{02})=Gr\vartheta-\left(E_1\frac{\partial^3 h}{\partial x^3}+E_2\frac{\partial^3 h}{\partial x\partial t^2}+E_3\frac{\partial^2 h}{\partial x\partial t}\right)\end{aligned} \tag{46}$$

$$(1-\alpha\vartheta)\frac{\partial^2}{\partial y^2}(u_{10}+\alpha u_{11}+\alpha^2 u_{12})+2(1-\alpha\vartheta)\frac{\partial^2 u_0}{\partial y^2}\frac{\partial}{\partial y}(u_{00}+\alpha u_{01}+\alpha^2 u_{02})-\alpha\frac{\partial\vartheta}{\partial y}\frac{\partial}{\partial y}(u_{10}+\alpha u_{11}+\alpha^2 u_{12})$$
$$-\alpha\frac{\partial\vartheta}{\partial y}\left(\frac{\partial}{\partial y}(u_{00}+\alpha u_{01}+\alpha^2 u_{02})\right)^2+\left[M^2+\frac{1}{Da}(1-\alpha\vartheta)\right](u_{10}+\alpha u_{11}+\alpha^2 u_{12})=0 \quad (47)$$

$$(1-\alpha\vartheta)\frac{\partial^2}{\partial y^2}(u_{20}+\alpha u_{21}+\alpha^2 u_{22})+2(1-\alpha\vartheta)\left\{\begin{array}{l}\left(\frac{\partial^2}{\partial y^2}(u_{10}+\alpha u_{11}+\alpha^2 u_{12})\right)\left(\frac{\partial}{\partial y}(u_{00}+\alpha u_{01}+\alpha^2 u_{02})\right)\\+\frac{\partial^2}{\partial y^2}(u_{00}+\alpha u_{01}+\alpha^2 u_{02})\left(\frac{\partial}{\partial y}(u_{10}+\alpha u_{11}+\alpha^2 u_{12})\right)\end{array}\right\}$$
$$-\alpha\frac{\partial\vartheta}{\partial y}\left\{\frac{\partial}{\partial y}(u_{20}+\alpha u_{21}+\alpha^2 u_{22})+2\left(\frac{\partial}{\partial y}(u_{10}+\alpha u_{11}+\alpha^2 u_{12})\right)\left(\frac{\partial}{\partial y}(u_{00}+\alpha u_{01}+\alpha^2 u_{02})\right)\right\}$$
$$+\left[M^2+\frac{1}{Da}(1-\alpha\vartheta)\right](u_{20}+\alpha u_{21}+\alpha^2 u_{22})=0 \quad (48)$$

The solutions of equations (46)-(48), and the corresponding stream functions, are a very long. The attendant constants can be determinate by using the boundary conditions given in (43)-(44).

Finally, the perturbation solutions up to second term for *u* and ψ are given by:

$$u=(u_{00}+\alpha u_{01}+\alpha^2 u_{02})+We(u_{10}+\alpha u_{11}+\alpha^2 u_{12})+We^2(u_{20}+\alpha u_{21}+\alpha^2 u_{22}) \quad (49)$$

$$\psi=(\psi_{00}+\alpha\psi_{01}+\alpha^2\psi_{02})+We(\psi_{10}+\alpha\psi_{11}+\alpha^2\psi_{12})+We^2(\psi_{20}+\alpha\psi_{21}+\alpha^2\psi_{22}) \quad (50)$$

5. Results and discussion

In this section, the numerical and computational results are discussed for the problem of an incompressible non-Newtonian the peristaltic flow of a Williamson fluid model through porous medium under combined effects of MHD and wall properties through the graphical illustrations. The numerical evaluations of the analytical results and some important results are displayed graphically in Figures- (2-15). MATHEMATICA program is used to find out numerical results and illustrations. The analytical solutions of the momentum equation are obtained by using perturbation technique. All the obtained solutions are discussed graphically under the variations of various pertinent parameters in the present section. The trapping bolus phenomenon is also incorporated through sketching graphs of streamlines for various physical parameters.

Based on equation (49), Figures (2-5) illustrates the effects of the parameters E_1, E_2, E_3, *We*, *Gr*, β, *M*, *Da* and ϕ on the velocity. Figure-2 illustrates the effects of the parameters E_1 and E_2 on the velocity distribution function u vs. y. It is found that the velocity profile *u* rising up with the increasing effects of both the parameters E_1 and E_2, when $|y|$ < 0.8643, and attains its maximum height at *y* = 0, the fluid velocity starts increasing and tends to be constant at the peristaltic walls, as specified by the boundary conditions. From Figure-3 One can depict here that velocity decreases with increasing of E_3, while that velocity profile is rising up with increasing of the parameters *We*, when $|y|$ < 0.8643. Figure-4 contains the behavior of *u* under the variation of *Gr* and β, one can depict here that *u* go down with the increasing effects of both the parameters *Gr* and β, when $|y|$ < 0.8643. Figure-5 illustrates the effects of the parameters *M* and *Da* on velocity profile. One can depict here that velocity decreases with increasing of *Da*, while that velocity profile is rising up with increasing of*M*, when $|y|$ <0.8643. Figure-6 show that velocity distribution decreases with an increasing of ϕ. Also at ϕ = 0.15, *u* > 0 when $|y|$ < 0.8643 and *u*(0.8643) = 0. At ϕ = 0.175, *u* > 0 when $|y|$ < 0.8417 and *u*(0.8417) = 0, as specified by the boundary conditions.

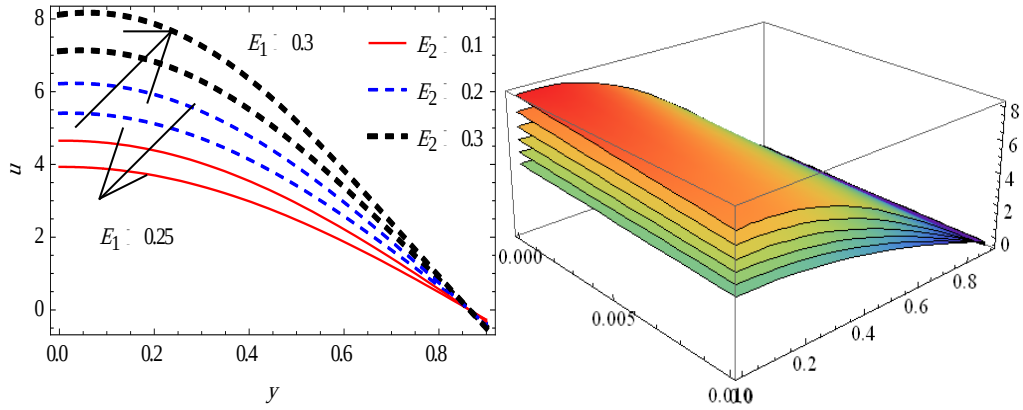

Figure 2- Velocity profile for different values of E_1 and E_2 with $x=0, t=0.1, We=0.05, \alpha=0.02, E_3=0.1, Gr=1, \phi=0.15, \beta=1, Da=0.7, M=0.9$.

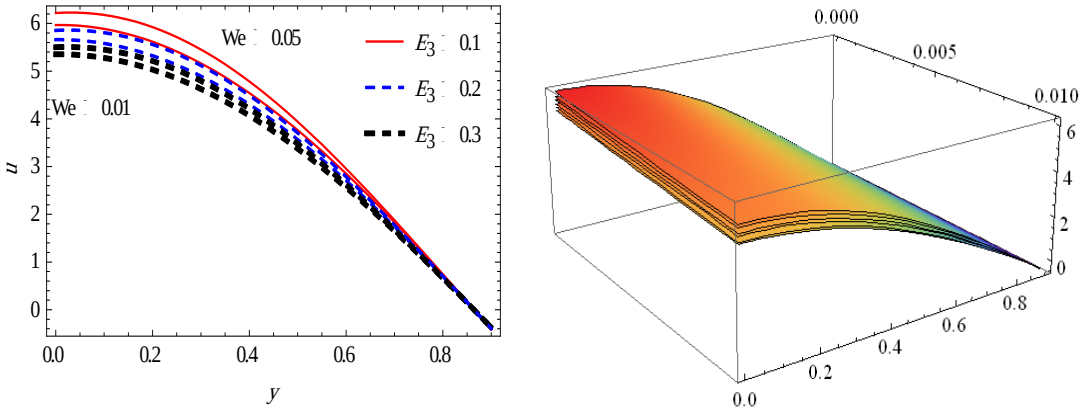

Figure 3- Velocity profile for different values of *We* and E_3 with $x=0, t=0.1, \alpha=0.02, E_1=0.3, E_2=0.2, \phi=0.15, Gr=1, \beta=1, Da=0.7, M=0.9$

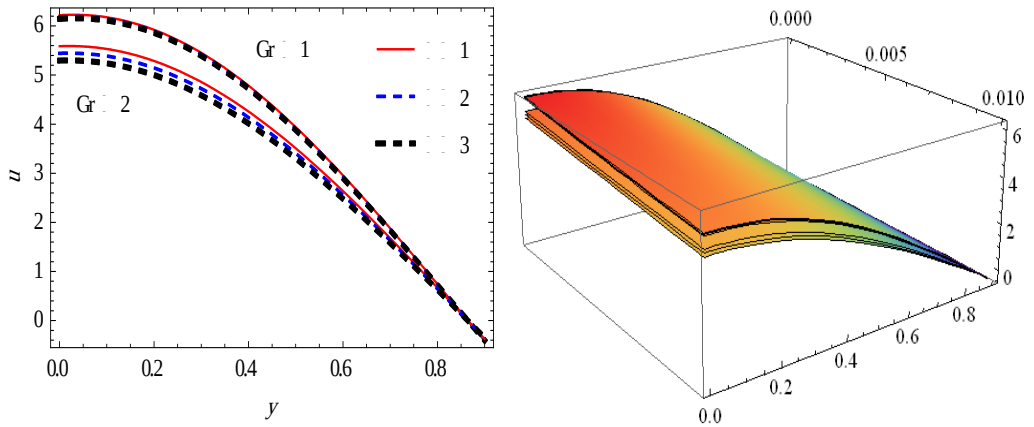

Figure 4- Velocity profile for different values of Gr and β with $x=0, t=0.1, We=0.05, \alpha=0.02, E_1=0.3, E_2=0.2, E_3=0.1, \phi=0.15, Da=0.7, M=0.9$

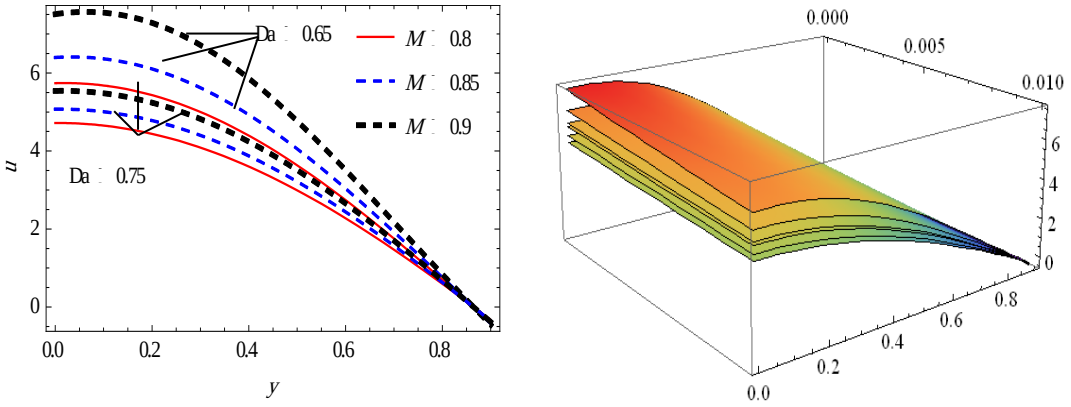

Figure 5- Velocity profile for different values of *Da* and *M* with
$x = 0, t = 0.1, We = 0.05, \alpha = 0.02, E_1 = 0.3, E_2 = 0.2, E_3 = 0.1, \phi = 0.15, Gr = 1, \beta = 1$

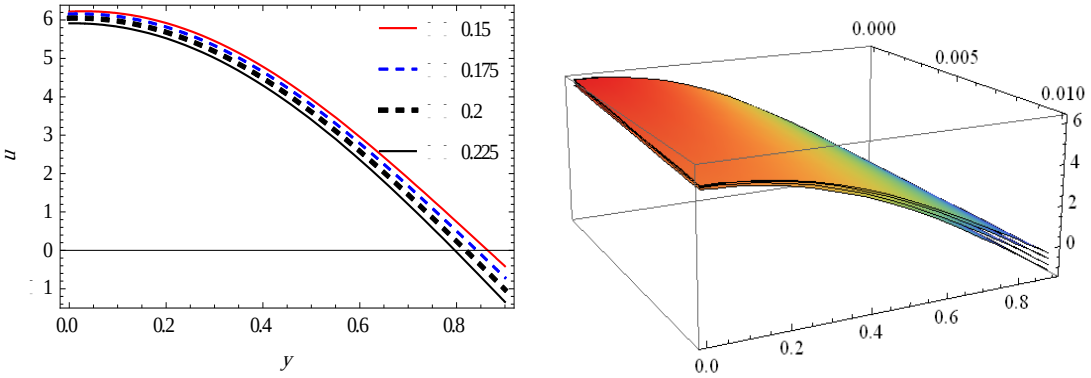

Figure 6- Velocity profile for different values of ϕ with
$x = 0, t = 0.1, We = 0.05, \alpha = 0.02, E_1 = 0.3, E_2 = 0.2, E_3 = 0.1, Gr = 1, \beta = 1, Da = 0.7, M = 0.9$

6. Trapping phenomenon

The formation of an internally circulating bolus of fluid by closed streamlines is called trapping and this trapped bolus is pushed ahead along with the peristaltic wave.

Based on equation (50), the effects of E_1, E_2, E_3, *Gr*, β, *Da*, *M*, *We* and ϕ on trapping can be seen through Figures- (7-15), it is observed that the bolus move near the side walls. Figure-7 shows that the size of the trapped bolus increase with the increase in E_1. Figure-8 is plotted, the effect of E_2 on trapping, the size of the trapped bolus increase with the increase in E_2. Figure-9 shows that the size of the left trapped bolus increases with increase in E_3 whereas the size of the right trapped bolus decreases with increase in E_3. The effect of *Gr* on trapping is analyzed in Figure-10. It can be concluded that the size of the trapped bolus in the left side of the channel decreases when *Gr* increases where as it has opposite behavior in the right-hand side of the channel. Figure-11 shows that the size of the trapped bolus increases with increase in β. The influence of *Da* on trapping is analyzed in Figure-12. It shows that the size of the trapped bolus decreases with increase in *Da*. Figure-13 shows that influence of *M* on trapping. It shows that the size of the trapped bolus increases with increase in *M*. The influence of *We* on trapping is analyzed in Figure-14. It shows that the size of the trapped bolus increases with increase in *We*. And the effect of ϕ on trapping is analyzed in igure-15. We notice that the size of the trapped bolus increases with increase ϕ.

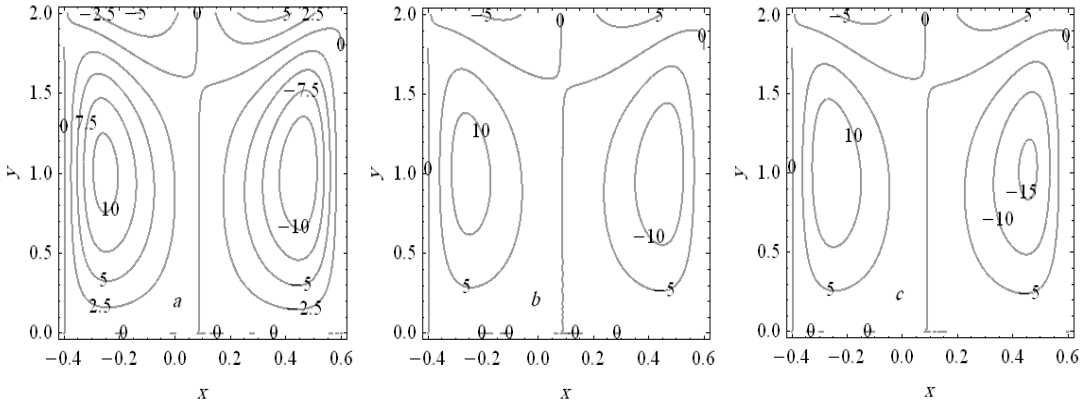

Figure 7- Graph of the streamlines for three different values of E_1; (a) E_1 = 0.25, (b) E_1 = 0.3 and (c) E_1 = 0.35 at $t = 0.1, We = 0.05, \alpha = 0.02, E_2 = 0.2, E_3 = 0.1, Da = 0.8, M = 0.9, Gr = 1, \phi = 0.15, \beta = 1$.

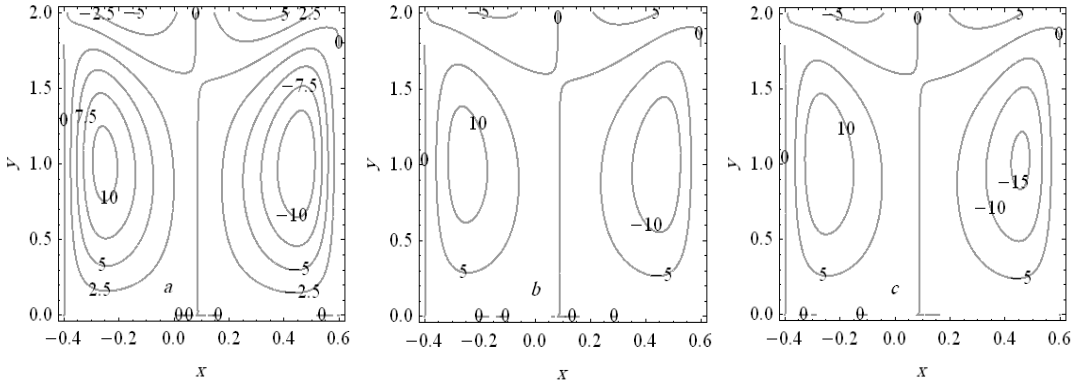

Figure 8- Graph of the streamlines for three different values of E_2; (a) E_2 = 0.15, (b) E_2 = 0.2 and (c) E_2 = 0.25 at $t = 0.1, We = 0.05, \alpha = 0.02, E_1 = 0.3, E_3 = 0.1, Da = 0.8, M = 0.9, Gr = 1, \phi = 0.15, \beta = 1$.

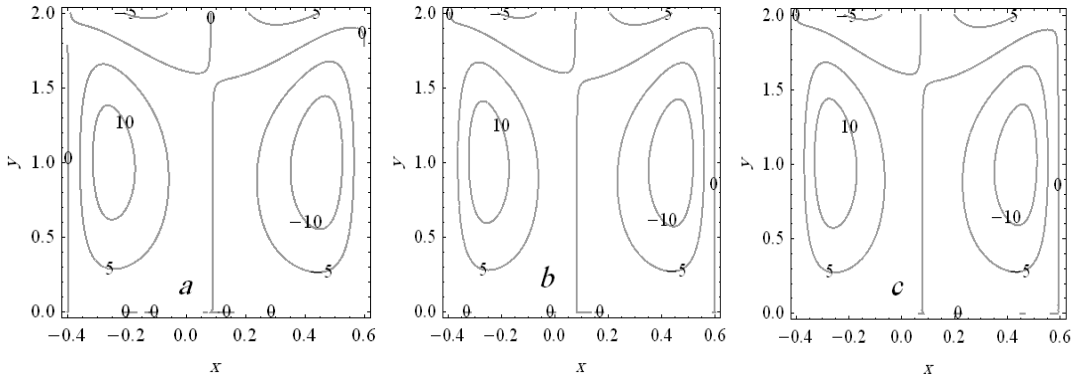

Figure 9- Graph of the streamlines for three different values of E_3; (a) E_3 = 0.1, (b) E_3 = 0.2 and (c) E_3 = 0.3 at $t = 0.1, We = 0.05, \alpha = 0.02, E_1 = 0.3, E_2 = 0.2, Da = 0.8, M = 0.9, Gr = 1, \phi = 0.15, \beta = 1$.

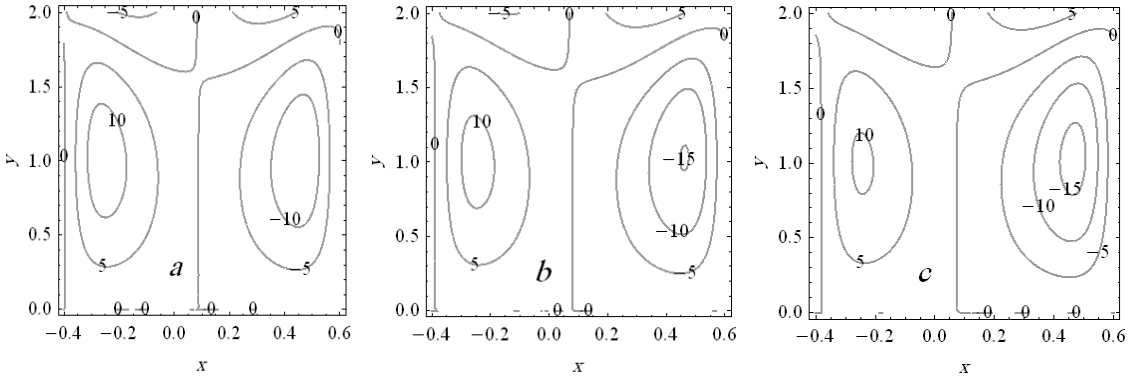

Figure 10- Graph of the streamlines for three different values of *Gr* ; (a) *Gr* = 1, (b) *Gr* = 2 and (c) *Gr* = 3 at $t = 0.1, We = 0.05, \alpha = 0.02, E_1 = 0.3, E_2 = 0.2, E_3 = 0.1, Da = 0.8, M = 0.9, \phi = 0.15, \beta = 1$.

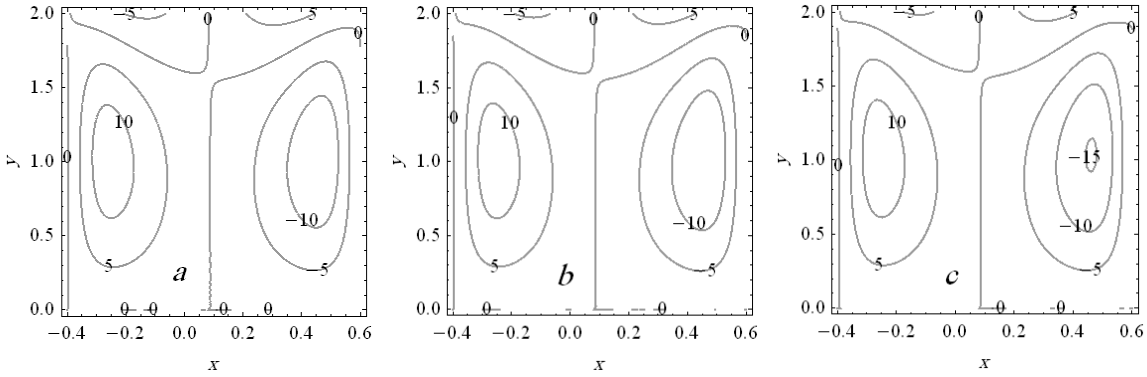

Figure 11- Graph of the streamlines for three different values of β ; (a) β = 1, (b) β = 2 and (c) β = 3 at $t = 0.1, We = 0.05, \alpha = 0.02, E_1 = 0.3, E_2 = 0.2, E_3 = 0.1, Da = 0.8, M = 0.9, Gr = 1, \phi = 0.15$.

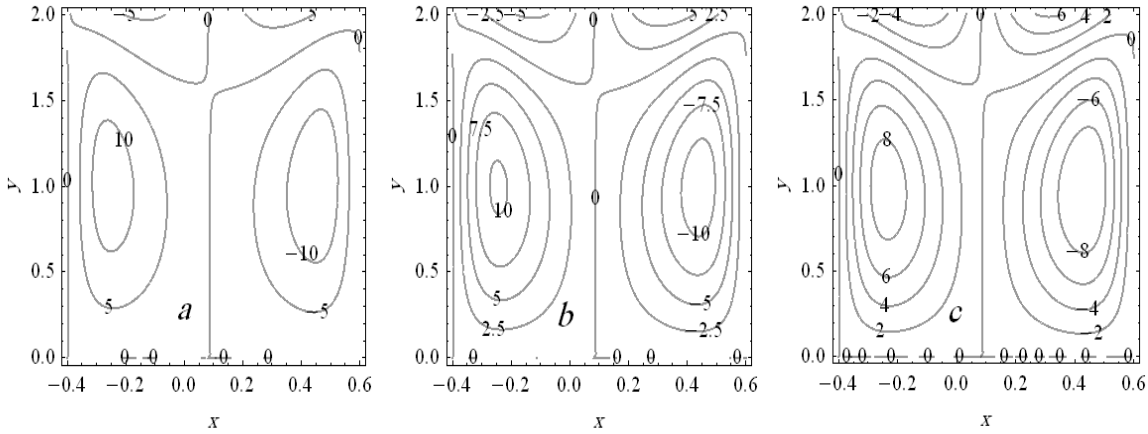

Figure 12- Graph of the streamlines for three different values of *Da*; (a) *Da* = 0.8, (b) *Da* = 0.85 and (c) *Da* = 0.9 at $t = 0.1, We = 0.05, \alpha = 0.02, E_1 = 0.3, E_2 = 0.2, E_3 = 0.1, M = 0.9, Gr = 1, \phi = 0.15, \beta = 1$.

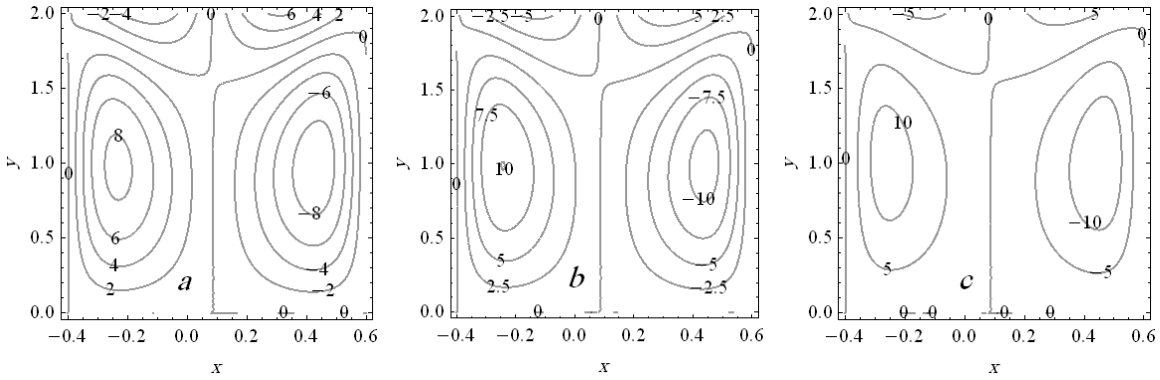

Figure 13- Graph of the streamlines for three different values of *M*; (a) *M* = 0.8, (b) *M* = 0.85 and (c) *M* = 0.9 at $t = 0.1, We = 0.05, \alpha = 0.02, E_1 = 0.3, E_2 = 0.2, E_3 = 0.1, Da = 0.8, Gr = 1, \phi = 0.15, \beta = 1$.

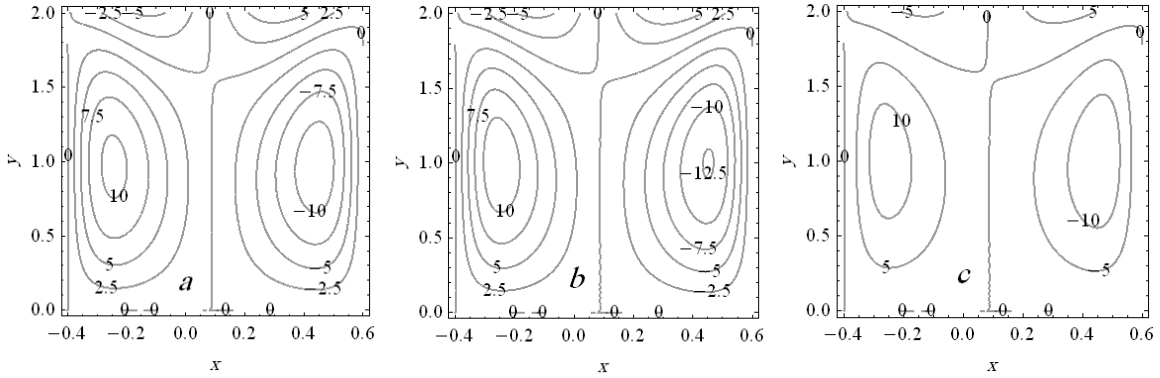

Figure 14- Graph of the streamlines for three different values of *We*; (a) *We* = 0, (b) *We* = 0.025 and (c) *We* = 0.05 at $t = 0.1, E_1 = 0.3, E_2 = 0.2, E_3 = 0.1, Gr = 1, Da = 0.8, M = 0.9, \phi = 0.15, \beta = 1$.

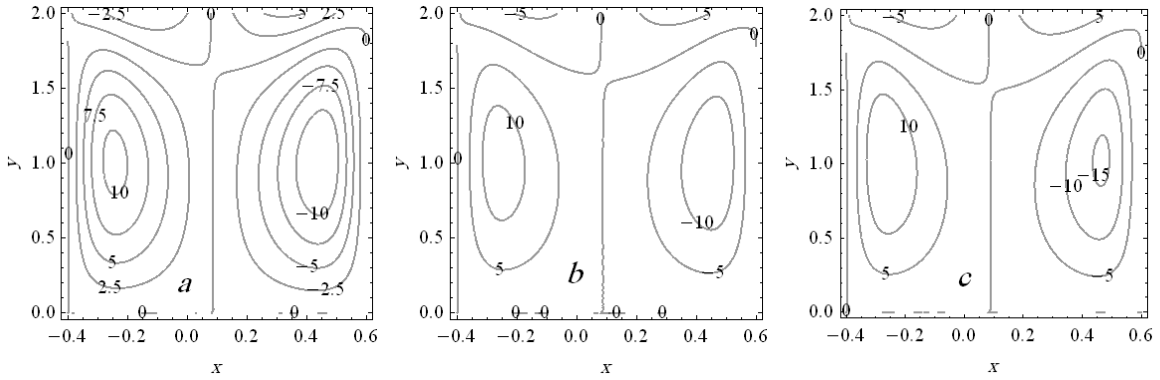

Figure 15- Graph of the streamlines for three different values of ϕ; (a) ϕ = 0.125, (b) ϕ = 0.15 and (c) ϕ = 0.175 at $t = 0.1, We = 0.05, E_1 = 0.3, E_2 = 0.2, E_3 = 0.1, Da = 0.8, M = 0.9, Gr = 1, \beta = 1$.

7. Concluding remarks

The present study deals with the combined effect of MHD and wall properties on the peristaltic transport of a Williamson fluid in a two-dimensional channel through porous medium. We obtained the analytical solution of the problem under long wavelength and low Reynolds number assumptions. The results are analyzed for different values of pertinent parameters namely Grashof number, Darcy number, thermal conductivity, rigidity, stiffness, magnet and viscous damping forces of the channel wall through porous medium. From wall properties and type of fluid (Williamson), we observed that the bolus moves near the side walls. The main findings can be summarized as follows:

1. The axial velocity increases with the increase in E_1, E_2, *We* and *M*, when $|y| < 0.8643$. Further, the axial velocity decreases with increase in E_3, *Gr*, β, *Da* and ϕ.
2. The size of the trapped bolus increases with the increase in E_1, E_2, *M*, ϕ, β and *We*. While the size of the trapped bolus decreases with increase in *Da*.
3. The size of the left trapped bolus increases with increase in E_3 whereas it has opposite behavior in the right hand side of the channel. And the size of the trapped bolus in the left side of the channel decreases when *Gr* increases where as it has opposite behavior in the right hand side of the channel.
4. The comparison between the effects of various viscosities on Williamson fluid. The velocity for Williamson fluid with constant viscosity is more than velocity of Williamson fluid with variable viscosity, and attains its maximum height at y = 0, moreover the fluid velocity starts increasing and tends to be constant at the peristaltic walls. The real values of stream function for Williamson fluid with constant viscosity is more than the real values of stream function for Williamson fluid with variable viscosity for the same values of the parameters. And the variation of trapped bolus for Williamson fluid with constant viscosity is more than the variation for trapped bolus of Williamson fluid with variable viscosity when to change the effect parameters, see [25] for details.

References

1. Latham, T.W. **1966**. Fluid motions in peristaltic pump, M.S. Thesis, *MIT*, Cambridge, Massachussetts.
2. Shapiro, A.H., Jaffrin, M.Y and Weinberg, S.L. **1969**. Peristaltic pumping with long wavelengths at low Reynolds number. *J. Fluid Mech*. **37:** 799-825.
3. Fung, Y.C. and Yih, C. S. **1968**. Peristaltic transport. *Trans. ASME J. Appl. Mech*., **35**: 669-675.
4. Brown.T.D, and Hung.T.K. **1977**. Computational and experimental investigations of two-dimensional nonlinear peristaltic flows, *J. Fluid Mech*., **83**: 249-272.
5. Takabatake, S., Ayukawa, K. and Mori, A. **1988**. Peristaltic pumping in circular tubes: A numerical study of fluid transport and its efficiency. *J. Fluid Mech*., **193**: 267-283.
6. Ramachandra, Rao, A., and Usha, S. **1995**. Peristaltic transport of two immiscible viscous fluid in a circular tube. *J. Fluid Mech*., **298:** 271-285.
7. Siddiqui, A.M., Provost, A. and Schwarz, W.H. **1991**. Peristaltic pumping of a second- order fluid in a planar channel. *Rheol. Acta.* **30:** 249-262.
8. Siddiqui, A.M. and Schwarz, W.H. **1994**. Peristaltic flow of a second order fluid in tubes. *J. Non-Newtonian Fluid Mech*., **53**: 257-284.
9. Siddiqui, A.M., Provost, A. and Schwarz, W.H. **1993**. Peristaltic pumping of a third- order fluid in a planar channel. *Rheol.Acta*, **32**: 47-56
10. Hayat, T., Wang, Y., Siddiqui, A.M., Hutter, K. and Asghar, S. **2002**. Peristaltic transport of a third-order fluid in a circular cylindrical tube. *Math. Models & Methods in Appl. Sci*., **12**: 1691-1706
11. Haroun, M.A. **2007**. Effects of Deborah number and phase difference on peristaltic transport of a third – order fluid in an asymmetric channel. *Comm. Nonlinear Sic.Nuber. Simul*., **12**: 1464 -1480.
12. Nadeem, S. and Akram, S. **2010**. Peristaltic flow of a Williamson fluid in an asymmetric channel. *Comm. Nonlinear sic. Numer. Simul*., **15**: 1705 –1716.
13. Mitra, T. K. and Prasad S. N. **1973**. On the influence of wall properties and Poiseuille flow in peristalsis. *Journal of Biomechanics*, **6**: 681-693.
14. Mishra, JC. and Pandey, SK. **2001**. A Mathematical Model for Oesophageal Swallowing of a Food Bolus. *Mathematical and Computer Modelling*, **33**: 997-1009.
15. Rathod, V. P. and Pallavi, K. **2011**. The Influence of Wall Properties on MHD Peristaltic transport of Dusty Fluid. *Advances in applied Science Research*, **2**(3): 265-279.
16. Radhakrishnamacharya, G. and Srinivasulu, Ch. **2007**. Influence of wall properties on peristaltic transport with heat transfer. *Computer Rendus Mecanique*, **335**: 369-373.
17. Rathod, VP. and Pallavi, Kulkarni. **2011**. The Influence of Wall Properties on MHD Peristaltic transport of Dusty Fluid *Advances in applied Science Research*, **2**(3): 265-279.

18. Mokhtar, A. Abd Elnaby and Haroun, MH. **2008**. A new model for study the effect of wall properties on peristaltic transport of a viscous fluid. *Communication in Nonlinear Science and Numerical simulation*, **13**: 752-762.
19. Srinivas, S., Gayathri, R. and Kothandapani, M. **2009**. The influence of slip conditions, wall properties and heat transfer on MHD peristaltic transport. *Computer Physics Communications*, **180** (11): 2115–2122.
20. Al-Khafajy, Dheia, Abdulhadi, A. M. 2014. Effects of wall properties and heat transfer on the peristaltic transport of a Jeffrey fluid through porous medium channel. *Mathematical Theory and Modeling–IISTE*, **4**(9): 86-99.
21. Al-Khafajy, Dheia, Abdulhadi, A. M. **2014**. Effects of MHD and wall properties on the peristaltic transport of a Carreau fluid through porous medium, *Journal of Advances in Physics*, **6**(2): 1106-1121.
22. Al-Khafajy, Dheia, Abdulhadi, A. M. **2015**. Influence of wall properties and heat transfer on the peristaltic transport of a Williamson fluid through porous medium channel, *IJARSET*, **2**(11): 970-981.